

Direct Simulation Monte Carlo Investigation of Hydrodynamic Instabilities in Gases

M. A. Gallis,^{1,a)} T. P. Koehler,^{1,b)} J. R. Torczynski,^{1,c)} S. J. Plimpton^{2,d)}

¹*Engineering Sciences Center, Sandia National Laboratories,
P. O. Box 5800, Albuquerque, New Mexico 87185-0840 USA*

²*Computing Research Center, Sandia National Laboratories,
P. O. Box 5800, Albuquerque, New Mexico 87185-1316*

^{a)}Corresponding author: magalli@sandia.gov

^{b)}tkoehle@sandia.gov, ^{c)}jrtorcz@sandia.gov, ^{d)}sjplimp@sandia.gov

Abstract. The Rayleigh-Taylor instability (RTI) is investigated using the Direct Simulation Monte Carlo (DSMC) method of molecular gas dynamics. Here, two-dimensional and three-dimensional DSMC RTI simulations are performed to quantify the growth of flat and single-mode-perturbed interfaces between two atmospheric-pressure monatomic gases. The DSMC simulations reproduce all qualitative features of the RTI and are in reasonable quantitative agreement with existing theoretical and empirical models in the linear, nonlinear, and self-similar regimes. At late times, the instability is seen to exhibit a self-similar behavior, in agreement with experimental observations. For the conditions simulated, diffusion can influence the initial instability growth significantly.

INTRODUCTION

A large number of important engineering and scientific problems involve flow instabilities, i.e., flows in which naturally occurring infinitesimal disturbances amplify spontaneously and ultimately dominate the flows. To analyze such a flow, linear stability theory¹ considers sinusoidal disturbances on the initial state of the fluid and tracks their evolution with time. Instabilities are complicated because they involve a large number of degrees of freedom and they become nonlinear when the disturbances become large. Baroclinic instabilities occur when density and pressure gradients are misaligned. In meteorological flows, baroclinic instabilities are the most important mechanism for generating low-pressure cyclonic circulations, so they strongly influence weather generation in the middle latitudes¹.

Herein, Bird's Direct Simulation Monte Carlo (DSMC) method² of molecular gas dynamics is employed to simulate baroclinic instabilities triggered not only by sinusoidally perturbed interfaces but also by naturally occurring thermal fluctuations in gases, which are typically ignored in continuum fluid mechanics. In particular, the Rayleigh-Taylor instability (RTI) at the interface between two gases is investigated.

The RTI evolves at the unstable interface of two fluids of different densities subjected to a common acceleration normal to the interface. In this situation, small interfacial perturbations evolve into mushroom-like structures with wavelength λ and amplitude a that both increase as time progresses. Taylor³ conducted the original theoretical study of the RTI, and Lewis⁴ conducted the companion experimental study. Since then, many sophisticated theoretical, numerical, and experimental studies have been conducted to quantify the behavior of the RTI. Extensive reviews of the more recent research on the RTI can be found in Sharp⁵, Kull⁶, and Abarzhi⁷.

For miscible fluids subject to a constant acceleration, the RTI can be described as having three fundamentally different phenomenological stages of mixing: linear, nonlinear, and turbulent. In the first stage, small initial perturbations on the interface grow exponentially. In this stage, the growth dynamics can be described by two length

scales: the perturbation amplitude a in the acceleration direction and the perturbation wavelength λ , which is related to the mode of fastest growth (i.e., the most unstable wavelength, λ_m).

In the second stage, larger coherent structures appear as smaller disturbances interact and merge. These interactions occur when the perturbation amplitude becomes comparable to the perturbation wavelength. In this stage, the amplitude growth follows a power law with time. In the third stage, secondary instabilities like the Kelvin-Helmholtz instability develop and eventually break up the coherent structures, which results in turbulent and chaotic mixing of the fluids.

The details of the evolution of the RTI clearly depend on the properties of the two fluids. By broadening the density transition between the gases⁸, viscosity and diffusivity inhibit small-wavelength perturbations from growing, thereby allowing a particular wavelength (the most unstable wavelength λ_m) to emerge, whose growth outpaces the growth of all other wavelengths. Diffusion can also reduce the effective buoyant forces, thus slowing the mixing process.

As a result, for an initially flat interface, the most unstable wavelength has the following form⁵: $\lambda_m \approx 4\pi(v^2/Ag)^{1/3}$, where g is the gravity (acceleration) to which the domain is subjected, v is the mean kinematic viscosity of the two fluids, $A = (\rho_H - \rho_L)/(\rho_H + \rho_L)$ is the Atwood number, and ρ_H and ρ_L are the densities of the heavy and light fluids, respectively. Other factors that have been shown to influence the growth of the instability include the dimensionality of the flow, the time dependence of gravity, and boundary effects. It is also common to utilize length and time scales based upon gravity and the initial perturbation wavelength as a means to analyze the data. A typical time scale associated with the growth of the instability is $\tau \sim 1/\sqrt{Agk}$, where the wavenumber is related to the wavelength according to $k = 2\pi/\lambda$.

In this paper, DSMC is used to investigate the growth of the RTI as the initial perturbation and the dimensionality of the flow are varied over six simulations (see Table 1). Two-dimensional and three-dimensional DSMC RTI simulations are performed for monatomic gases at essentially atmospheric conditions. The first four simulations are two-dimensional. In these simulations, the gravitational acceleration g and the Atwood number A are fixed by using argon and helium, but the initial perturbation wavelength λ is varied. These simulations all employ an initial perturbation amplitude a_0 that is 1% of the initial perturbation wavelength λ . In the fifth simulation, all conditions are the same as in the first simulation, except that the initial interface is molecularly flat (i.e., the initial amplitude a_0 is zero). Finally, the sixth simulation repeats the conditions of the fifth except that the simulation is three-dimensional rather than two-dimensional.

Linear stability theory determines when a flow is unstable to infinitesimal disturbances. Infinitesimal disturbances, caused by thermal fluctuations in the gas, are always present even for a molecularly flat surface. Rayleigh⁸ first studied the stability of the interface between two fluids under the influence of a gravitational field, and Taylor¹ subsequently added an acceleration induced by pressure gradients. According to Taylor's linear stability theory, initial perturbations with small wavelengths grow faster, where a is the perturbation amplitude:

$$a = a_0 \cosh\left(t\sqrt{Agk}\right), \quad k = 2\pi/\lambda. \quad (1)$$

Equation (1) suggests that smaller wavelengths always result in larger growth rates. When the effects of viscosity and diffusivity are included, the growth of the instability amplitude is modified⁸:

$$a = a_0 \exp\left(\left[(Agk/\psi + v^2k^4)^{1/2} - (v+D)k^2\right]t\right), \quad (2)$$

where $k = 2\pi/\lambda$ is the wavenumber for wavelength λ , v is the kinematic viscosity, D is the diffusivity, and ψ is a function of the Atwood number A . In this case, the exponent in Equation (2) has a maximum for some particular wavelength, namely the most unstable wavelength λ_m .

Experiments have confirmed that linear theory correctly accounts for the early-time evolution of the instability amplitude⁵⁻⁷. However, at later times, when $ka \sim 1$, the flow is more complicated and requires a nonlinear stability approach or an empirical analysis. The fluids mix at different rates on either side of the interface: the amplitude of the coherent structures that penetrate from the light fluid into the heavy fluid, known as bubbles, grows more slowly than the amplitude of the coherent structures that penetrate from the heavy fluid into the light fluid, known as spikes. Building on an earlier model of Layzer¹⁰ and based on a very large number of experimental and numerical results, Mikaelian¹¹ proposed a model for the bubble amplitude a^b :

$$a^b(A) = a_0 + \left(\frac{3+A}{3(1+A)k}\right) \ln\left(\cosh\left[t\frac{\sqrt{6gkA(1+A)}}{(3+A)}\right]\right). \quad (3)$$

Mikaelian¹¹ also proposed a model for the spike amplitude a^s that interpolates between the spike growth for Atwood numbers of 0 and 1:

$$a^s(A) = a^b(A) \left(1 + \left[0.4 + 0.6A^{10} \right] \left[\left(\frac{a^s(1)}{a^b(A)} \right)^A - 1 \right] \right). \quad (4)$$

Here, a^s approaches a^b for $A \rightarrow 0$ but increases with A becoming 4-5 times a^b for $A \rightarrow 1$.

As the RTI develops further, the coherent structures begin to break down, and a self-similar turbulent mixing layer evolves. The existence of a self-similar regime for the RTI was first discussed by Fermi and von Neumann¹². In the turbulent regime, experimental data suggest that the bubble and spike growth rates are both self-similar¹³ and can be described by a relatively simple model: $a^{b,s} = \alpha^{b,s} A g t^2$, where $\alpha^{b,s}$ is a constant, usually between 0.03 and 0.07. However, α^s is not constant and depends on A . For the self-similar solution to be applicable, the instability amplitude must be greater than the viscous and diffusion scales. In practical terms, this means that the total instability growth $h = a^b + a^s$ must satisfy the condition $\lambda_m \ll h \ll L$, where L is the size of the physical domain.

Although the RTI has been treated successfully with hydrodynamic methods, recently, and with the advent of supercomputers, RTI flow fields have been simulated using molecular methods. The applicability of molecular methods to instability simulations has been investigated by Kadau et al.,^{14,15} Barber et al.,¹⁶ and Mościński et al.¹⁷ Their results suggest that, for liquids, molecular dynamics (MD) approaches can qualitatively and quantitatively describe the development of the RTI. In their results, the three stages of the instability are clearly observed as time progresses. The small initial perturbations evolve into larger spikes and bubbles, some showing turbulent shedding of vortices and eventually breaking completely apart. Kadau et al.^{14,15} further showed good agreement with experimental data for spike positions and velocities. Using a particle-based, kinetic Monte Carlo method, Sagert et al.¹⁸ also demonstrated good agreement with growth rates in the linear regime.

Recently, it was demonstrated¹⁹ that DSMC, can simulate baroclinic instabilities for the Richtmyer-Meshkov instability. Starting from a single-mode-perturbed interface, DSMC simulations produced results in agreement with expectations from numerical simulations, theory, and experiments.

Herein, the three-dimensional DSMC code SPARTA²⁰, developed to be highly efficient on massively parallel computers, is used to simulate the RTI in two-dimensional and three-dimensional millimeter-scale domains for atmospheric-pressure gases. Simulations are performed on Sequoia, an IBM Blue Gene/Q supercomputer at Lawrence Livermore National Laboratory, using up to 1.57 million cores for up to 30 hours, which yielded a maximum of 17 Pflops.

NUMERICAL ANALYSIS DETAILS

The DSMC code SPARTA²⁰ is used to simulate the RTI at the interface separating two gases experiencing a constant acceleration. The gases are dilute and obey the perfect-gas equation of state and are taken to have constant values of the specific heat ratio γ . These approximations are reasonable for the modest temperatures and pressures considered here.

The initial conditions consist of the heavier gas, argon (Ar), on top of the lighter gas, helium (He). The lighter gas is initially at 273.15 K and 101325 Pa (STP) at the bottom of the domain. Throughout the rest of the domain, both gases are initially at 273.15 K and have initial density distributions corresponding to hydrostatic equilibrium. The gases are accelerated by a constant gravity value of $g = 10^8 \text{ m/s}^2$.

For the two-dimensional simulations, a 1 mm \times 4 mm domain is used, and a sinusoidal perturbation with a wavelength of $\lambda = 1 \text{ mm}$ (equal to the domain width) and an amplitude of a_0 is initially imposed at the interface, which is located at $y = 2 \text{ mm}$. The domain is divided into 1.6 billion square cells with a side length of 50 nm, which is less than a mean free path at the interface for the gases considered. The domain is initialized in hydrostatic equilibrium with an average of 12.5 particles per cell, for a total of 20 billion particles. Due to the initial density gradient across the domain, most of the particles are initially concentrated in the lower half of the domain. With this particle density, the two-dimensional simulation can be considered as a thin (0.4 nm) three-dimensional domain in which each particle represents one real molecule. The molecular collisions are performed using the hard-sphere model with parameter values suggested by Gallis et al.²¹ The time step is 0.1 ns, which is less than both the mean collision time and the mean transit time of molecules in a cell.

RESULTS

In this section, DSMC simulations of two distinct RTI scenarios are presented. In the first scenario, an initial perturbation is imposed upon the interface with an amplitude $a_0 = \lambda/100$, so the instability grows initially in the linear regime and progresses into the early nonlinear regime. In the second scenario, the initial interface is flat (i.e., the amplitude is set to zero initially). At the molecular level, an interface cannot ever be mathematically flat. Thus, the effect of molecular fluctuations on instability growth is inherently observed. In both situations, DSMC results are obtained that can be quantitatively compared to the models discussed previously.

TABLE 1. Parameters for DSMC RTI simulations

Case	Gases	λ (mm)	a_0 (μm)	Dimensionality
1	Ar/He	1.00	10.0	2D
2	Ar/He	0.75	7.5	2D
3	Ar/He	0.50	5.0	2D
4	Ar/He	0.25	2.5	2D
5	Ar/He	1.00	0.0	2D
6	Ar/He	1.00	0.0	3D

Table 1 presents the conditions for all of the DSMC RTI simulations. In all calculations, the domain width is equal to the perturbation wavelength λ . Cases 1-4 investigate the effect of perturbation wavelength λ for fixed Atwood number A and gravitational acceleration g in two dimensions. Case 5 is identical to the first one, except that the initial amplitude a_0 is zero (the interface is initially molecularly flat). Case 6 is a three-dimensional simulation identical to Case 5. Since the product of the wave number $k = 2\pi/\lambda$ and the initial amplitude a_0 is much less than unity for all cases, the instability growth is initially linear (but ultimately becomes nonlinear).

Fig. 1 presents the mixing profiles for Cases 1-4. Each computational cell is colored according to the majority species in the cell. While all cases begin as single-mode perturbations, Cases 1-2 develop a multi-mode behavior as the interface evolves: secondary bubbles and spikes form, grow with time, begin to interact, and eventually merge. In some cases, the stems of the spikes get thinner with time, leading to the shedding of droplets during the last stages of development. In Cases 1-2, the numbers of secondary bubbles and spikes that arise are proportional to the numbers that would be observed based on the most unstable wavelength determined from average gas properties, as previously suggested. The secondary bubbles and spikes ultimately cause the single mode to become asymmetric. Unlike Cases 1-2, Cases 3-4 evolve in a single-mode fashion until the bubbles and spikes eventually diffuse into each other. In Cases 3-4, secondary bubbles and spikes do not appear because the most unstable wavelength is greater than or comparable to the domain width. However, even in Case 4, for which the growth is predominantly diffusive, the initial perturbation grows and possesses some of the characteristics of the first two cases.

Fig. 2 compares the bubble and spike amplitudes determined by DSMC simulations for Cases 1-4 to the results of linear theory and Mikaelian's theoretical model. To represent their directions of growth, the bubble amplitudes are shown as positive values, and the spikes are shown as negative values. The DSMC bubble growth is in excellent agreement with the linear theory until the amplitude grows to about twice the initial amplitude. At this point, the exponential growth is superseded by the power-law time-dependence in the nonlinear regime⁷. After the initial linear regime, the DSMC growth rate follows this trend, which is significantly lower than the growth rate predicted by linear theory but is very close to the growth rate predicted by Mikaelian's theory.

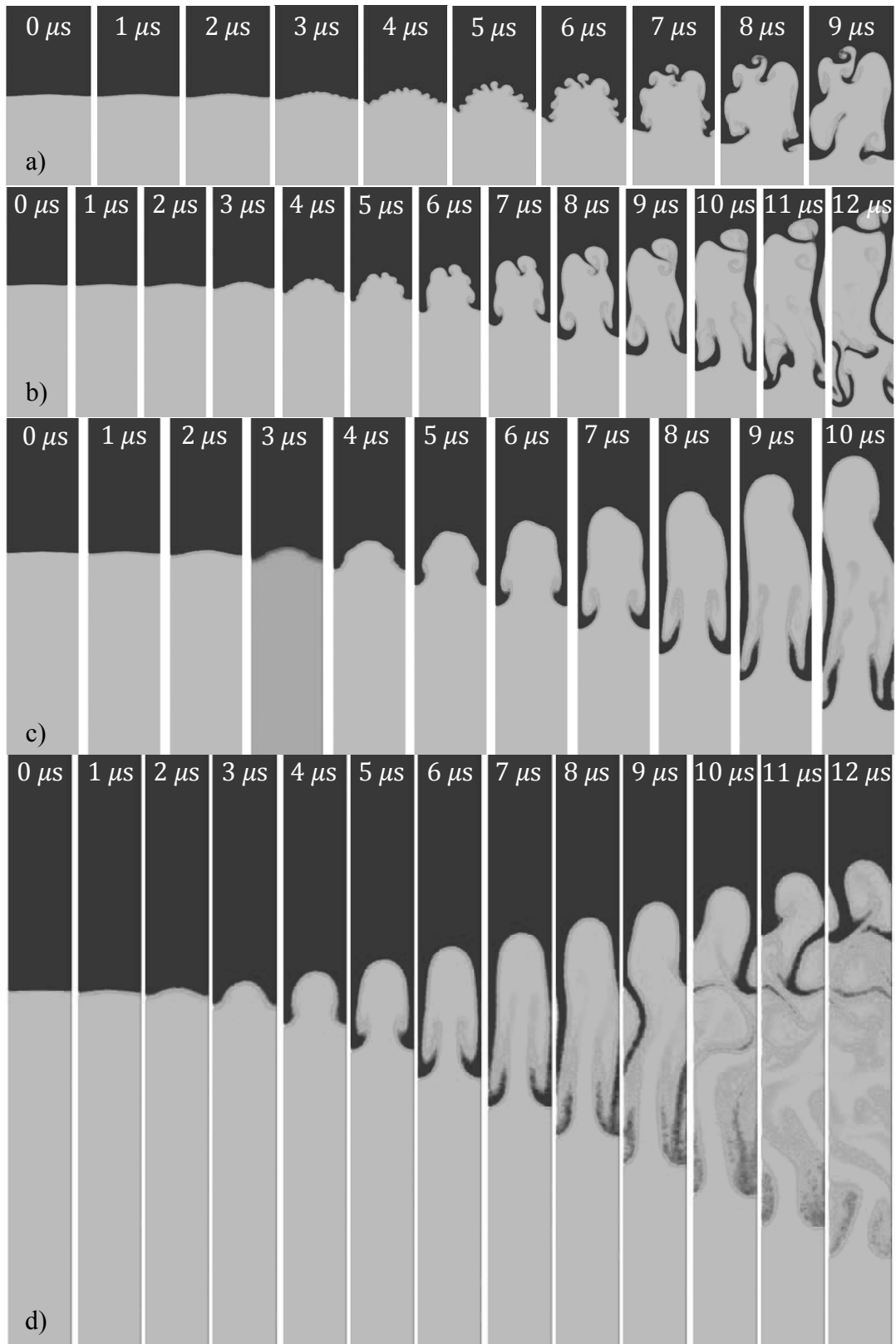


FIGURE 1. DSMC RTI simulations: Cases 1-4. Perturbation wavelength (top to bottom): a) 1.00, b) 0.75, c) 0.50, d) 0.25 mm.

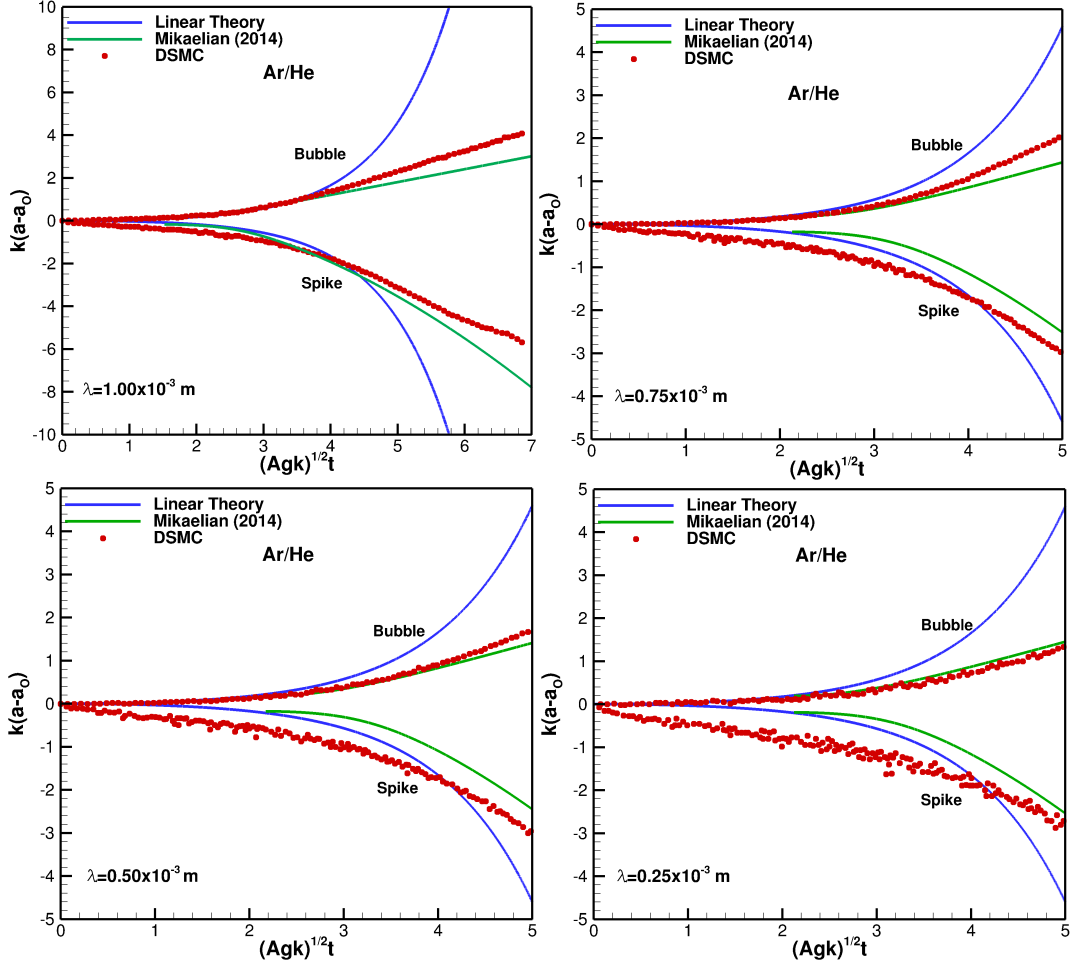


FIGURE 2. Effect of wavelength on amplitude growth for Cases 1-4.

One of the advantages of studying the RTI at the molecular level is that molecular techniques can initialize a simulation with a molecularly flat interface. This initial condition is hard, if not impossible, to achieve experimentally. Since fluctuations are absent, a simulation using a typical hydrodynamic method must be initialized with an artificially perturbed interface, often using the most unstable wavelength. In a molecular simulation, fluctuations excite all possible interfacial modes in a random fashion. In their molecular-dynamics simulations initialized with a flat interface, Kadau et al.¹⁴ observe that the unstable modes grow on average according to the predictions of linear stability theory.

Fig. 3 presents the mixing profile for Case 5. Although the interface is macroscopically flat in Case 5, it is perturbed microscopically on the length scale of inter-particle separations. As a result, in the absence of a macroscopic perturbation, molecular fluctuations become important to the development and growth of the instability. Perturbations with wavelengths near the most unstable wavelength will grow the most quickly. However, if no unstable wavelengths are produced, the interface will grow only by diffusion. The interface grows as the emerging bubbles and spikes become longer, begin interacting with each other, and eventually merge, which results in chaotic mixing. As in Cases 1-4, which have initially perturbed interfaces, the observed dominant wavenumber of the instability is approximately equal to the most unstable wavenumber in the light gas.

Fig. 4a presents the bubble and spike amplitude growth, defined as the distance between the initial position of the interface and the highest point of helium penetration into argon and the lowest point of argon penetration into helium, respectively, normalized using the most unstable wavelengths for the Ar/He mixture. The solid curves are curve fits for the self-similar regime. Here, Case 5 has $\alpha^b = 0.0382$ and $\alpha^s = 0.1050$. The bubble and spike values appear to be in line with expectations from experimental data^{13,23-25}.

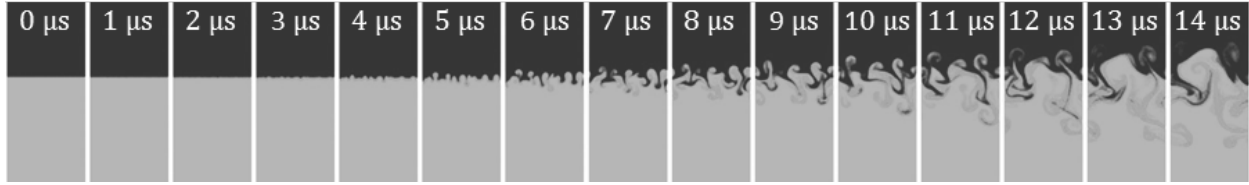


FIGURE 3. Two-dimensional DSMC RTI simulations. Domain width: 1.00 mm. Interface: initially flat. Gravity: 10^8 m/s^2 .

To confirm that this agreement is not affected by the two-dimensional nature of the simulation, the same simulation is repeated in three dimensions. The computational domain is a prism with a square cross section of $1 \text{ mm} \times 1 \text{ mm}$ and a height of 4 mm. The bubble and spike amplitudes are presented in Fig. 4b. For this case, the self-similarity coefficients are $\alpha^b = 0.0515$ and $\alpha^s = 0.1000$, which are in reasonable agreement with experimental observations. Instances of the density profile evolution as a function of time are given in Fig. 5. The initial mixing layer grows due to diffusion until the instability at the most unstable wavelength emerges.

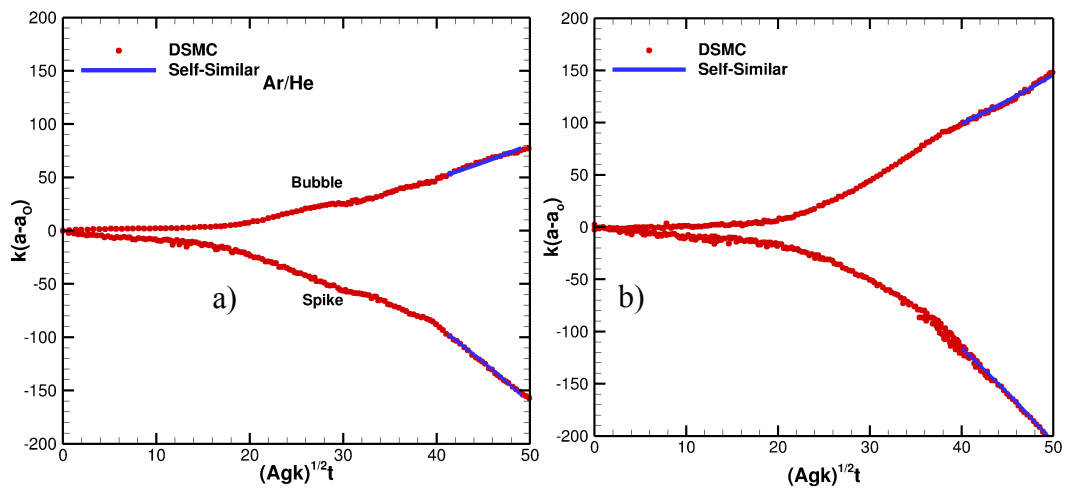


FIGURE 4. Amplitude growth for initially flat interfaces: Case 5 and Case 6.

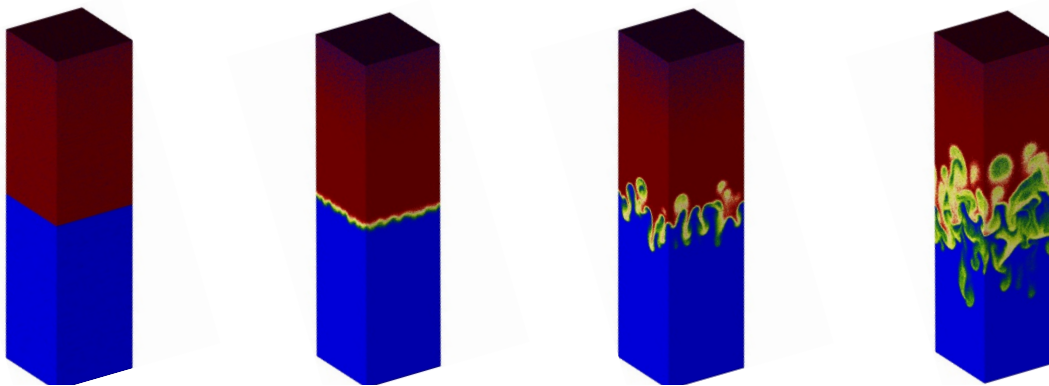


FIGURE 5. Three-dimensional DSMC RTI simulations. Times are 0, 4, 10, 14 μs .

CONCLUSIONS

DSMC simulations are performed to investigate the Rayleigh-Taylor instability (RTI). For initially perturbed interfaces, it is observed that diffusion can be a significant and sometimes dominant mixing process in early-time growth of the interface. The growth of the mixing region also shows that, although dominant in early times, diffusion does not affect the RTI significantly, thus justifying the simplifying assumptions often made in theoretical analyses of the RTI. For flat interfaces, it is demonstrated that the molecular nature of the DSMC simulations allows for the RTI to appear naturally, triggered by molecular fluctuations.

ACKNOWLEDGMENTS

Sandia National Laboratories is a multi-program laboratory managed and operated by Sandia Corporation, a wholly owned subsidiary of Lockheed Martin Corporation, for the U.S. Department of Energy's National Nuclear Security Administration under contract DE-AC04-94AL85000. The authors would like to thank Drs. D. J. Rader and S. N. Kempka of Sandia National Laboratories for many useful discussions and suggestions.

REFERENCES

1. J. C. Wyngaard, *Turbulence in the Atmosphere* (Cambridge University Press, Cambridge, 2010).
2. G. A. Bird, *Molecular Gas Dynamics and the Direct Simulation of Gas Flows* (Clarendon Press, Oxford, 1998).
3. G. I. Taylor, *Proceedings of the Royal Society of London. Series A, Mathematical and Physical Sciences*, 201 (1065), 192-196 (1950).
4. D. J. Lewis, *Proceedings of the Royal Society of London. Series A, Mathematical and Physical Sciences*, 202 (1068), 81-96 (1950).
5. D. H. Sharp, *Physica D: Nonlinear Phenomena*, 12 (1-3), 3-18 (1984).
6. F. Kull, *Physics Reports*, 206 (5), 197-325 (1991).
7. S. I. Abarzhi, *Philosophical Transactions of the Royal Society A*, 368, 1809-1828 (2010).
8. R. E. Duff, F. H. Harlow, and C. W. Hirt, *Physics of Fluids*, 5 (4), 417-425 (1962).
9. Lord Rayleigh, *Proceedings of the London Mathematical Society*, s1-14 (1), 170-177 (1883).
10. D. Layzer, *Astrophysical Journal*, 122 (1), 1-12 (1955).
11. K. O. Mikaelian, *Physical Review E*, 89 (05), 053009 (2014).
12. E. Fermi and J. von Neumann, *Technical Report AECU-2979*, Los Alamos Scientific Laboratory, Los Alamos, NM (1953).
13. A. W. Cook, W. Cabot, and P. L. Miller, *Journal of Fluid Mechanics*, 511, 333-362 (2004).
14. K. Kadau, J. L. Barber, T. C. Germann, B. L. Holian, and B. J. Alder, *Philosophical Transactions of the Royal Society A*, 368, 1547-1560 (2010).
15. K. Kadau, T. C. Germann, N. G. Hadjiconstantinou, P. S. Lomdahl, G. Dimonte, B. L. Holian, and B. J. Alder, *Proceedings of the National Academy of Science of the United States of America*, 101 (16), 5851-5855 (2004).
16. J. L. Barber, K. Kadau, T. C. Germann, P. S. Lomdahl, B. L. Holian, and B. J. Alder, *Journal of Physics: Conference Series*, 46, 58-62 (2006).
17. J. Mościński, W. Alda, M. Bubak, W. Dzwiniel, J. Kitowski, M. Pogoda, and D. A. Yuen, *Annual Reviews of Computational Physics*, V, 97-136, ed. D. Stauffer, (1997).
18. I. Sagert, J. Howell, A. Staber, T. Strother, D. Colbry, and W. Bauer, *Physical Review E*, 92 (01), 013009 (2015).
19. M. A. Gallis, T. P. Koehler, J. R. Torczynski, and S. J. Plimpton, *Physics of Fluids*, 27 (8), 084105 (2015).
20. S. J. Plimpton and M. A. Gallis, "SPARTA Direct Simulation Monte Carlo (DSMC) Simulator," <http://sparta.sandia.gov> (2015).
21. M. A. Gallis, J. R. Torczynski, and D. J. Rader, *Physical Review E*, 69 (4), 042201 (2004).
22. K. Kadau, J. L. Barber, T. C. Germann, and B. J. Alder, *Physical Review E*, 78, 045031 (2008).
23. W. H. Cabot and A. W. Cook, *Nature Physics*, 2, 562-568 (2006).
24. G. Dimonte and M. Schneider, *Physics of Fluids*, 12 (2), 304-321 (2000).
25. S. B. Dalziel, P. F. Linden, and D. L. Youngs, *Journal of Fluid Mechanics*, 399, 1-48 (1999).